
Change of Thought: Adaptive Test-Time Computation

Mrinal Mathur*
Google Research

Mike Doan†
TReNDS Center, Georgia State University

Barak A. Pearlmutter‡
Maynooth University

Sergey Plis†
TReNDS Center, Georgia State University

Abstract

Transformers evaluated in a single, fixed-depth pass are provably limited in expressive power to the constant-depth circuit class $TC \sim 0$. Running a Transformer autoregressively removes that ceiling—first in next-token prediction and, more recently, in chain-of-thought reasoning. Both regimes rely on feedback loops that decode internal states into tokens only to re-encode them in subsequent steps. While this “thinking aloud” mirrors human reasoning, biological brains iterate without externalising intermediate states as language. To boost the expressive power of encoder Transformers without resorting to token-level autoregression, we introduce the SELF-Transformer: an encoder layer that iteratively refines its own attention weights to a fixed point. Instead of producing—in one pass—the alignment matrix that remixes the input sequence, the SELF-Transformer iteratively updates that matrix internally, scaling test-time computation with input difficulty. This adaptivity yields up to 20% accuracy gains on encoder-style benchmarks without increasing parameter count, demonstrating that input-adaptive alignment at test time offers substantial benefits for only a modest extra compute budget. Self-Transformers thus recover much of the expressive power of iterative reasoning while preserving the simplicity of pure encoder architectures.

1 Introduction

The advent of transformers [1] has revolutionized natural language processing (NLP) and computer vision, achieving state-of-the-art results in language modeling, question answering, and image classification. At the core of their success lies the self-attention mechanism, which models long-range dependencies by dynamically computing input-dependent alignment matrices that determine how input tokens or patches are mixed. Transformers have achieved their widest success as large language models (LLM) through autoregressive operation that enabled success of large language models, first in next-token prediction [2] and more recently in chain-of-thought reasoning [3]. However, their reliance on token-level autoregression introduces inefficiencies: transformers repeatedly decode internal states into tokens and re-encode them in subsequent steps, creating computational bottlenecks. Unlike LLMs, the encoder transformers—the focus of this work—do not use causal attention and are widely used across a wide range of applications and models [4, 5, 6, 2, 7]. It is unclear whether autoregressive trick can be used to improve performance of these models. In common use, transformers remain powerful but rigid feedforward networks, that benefit from the external loop of their operation.

*Corresponding Author

†The Georgia State University/Georgia Institute of Technology/Emory University Center for Translational Research in Neuroimaging and Data Science (TReNDS Center).

‡Department of Computer Science, Maynooth University

To address these inefficiencies, recent work has explored dynamic computation networks [8], memory-augmented architectures [9, 10], and other mechanisms, as discussed in detail in §2. However, these approaches often trade simplicity for performance by introducing complex hypernetworks or external retrieval modules that inflate parameter counts and computational costs. Furthermore, while alignment matrices in conventional transformers are input-dependent and should account for input complexity, they are computed in a single feed-forward pass. This limits their ability to dynamically refine generated representations based on the obtained output.

In this work, we propose the Self-Enhancing Latent Feedback Transformer (SELF-Transformer), a novel architecture that augments self-attention (a) with Fixed-Point Iteration (FPI) to enable latent alignment refinement (Fig. 1).

Instead of generating alignment matrices in a single forward pass, SELF-Transformer iteratively updates them within the self-attention module. This iterative refinement process allows the model to dynamically adjust its attention patterns based on input complexity, spending more computational effort on challenging representations while maintaining efficiency for simpler inputs. By leveraging FPI universally across all layers, SELF-Transformer achieves deeper contextual reasoning without introducing additional parameters or task-specific modifications. Crucially, this approach enables SELF-Transformer to autoregressively improve its latent representations at each layer without the need to first decode them into tokens, all while incurring zero additional parameters.

An important property of Fixed-Point Self-Attention (FPSA) Fig. 1B is its focus on the iterative refinement of the layer’s parameters—the alignment matrix—rather than the output, which is more common in dynamic computation approaches (Fig. 1C&D). Although the end result similarly leads to an improvement in the output of the dynamic layer, FPSA explicitly operates on the dynamic parameters of that layer. Exploiting fixed-point iterations simplifies both the forward and backward paths during training, eliminating memory overhead during the process. This avoids the need for unrestricted memory consumption or checkpointing, which are often required in other dynamic computation methods.

2 Related Work

Dynamic Computation in Neural Networks The concept of dynamically adjusting computational effort based on input complexity has been a longstanding focus in machine learning. Early work by [11] introduced Adaptive Computation Time (ACT) for recurrent networks, allowing models to determine the number of computation steps per input. Stochastic depth networks [12] and early-exit architectures [13] later demonstrated that skipping layers or operations could improve efficiency without sacrificing accuracy. More recently, [14] formalized adaptive computation using learned halting distributions, while [15] proposed Mixture-of-Depths (MoD) to dynamically allocate compute across transformer layers. The Dynamic Diffusion Transformer (DyDiT) [16] further extends these ideas by dynamically adjusting computation along both timestep and spatial dimensions in diffusion models, achieving significant efficiency gains (see Fig. 1C for an example). Unlike these approaches, which often rely on auxiliary networks or heuristics, our method applies fixed-point iteration (FPI)

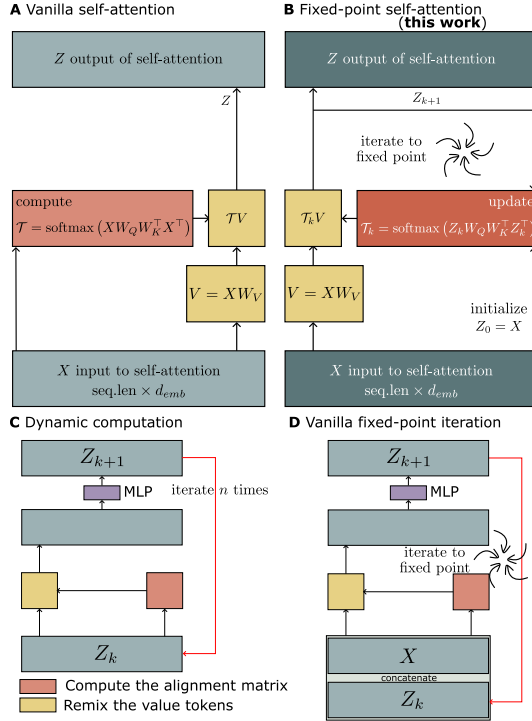


Figure 1: SELF-Transformer modifies vanilla self-attention (A) to iteratively update its alignment transform \mathcal{T} , adapting to the input sequence without introducing additional parameters (B). Compare with dynamic computation (C), which applies the same transformer block sequentially multiple times, and existing fixed-point iteration (D), which iterates the block to a fixed point.

universally within each layer as shown in Fig. 1B, enabling fine-grained refinement of self-attention alignments without introducing additional parameters.

Fixed-Point Methods in Deep Learning Fixed-point iteration has emerged as a powerful tool for modeling implicit depth in neural networks. Building on foundational work [17, 18, 19], and their more modern revival [20] methods like Deep Equilibrium Models (DEQs) [21] define infinite-depth networks through fixed-point equations. However, DEQs face challenges such as slow convergence and sensitivity to initialization [22], limiting their practicality. Recent advances address these issues via phantom gradients [23] and nonsmooth optimization techniques [24]. Complementary to these works, [25] conducted a detailed analysis of fixed-point iterations in high-dimensional neural networks, identifying conditions for convergence and stability. Our work diverges by applying FPI explicitly to self-attention matrices rather than complete layers, enabling iterative refinement of token alignments while maintaining gradient stability through implicit differentiation [26] as shown in Fig. 1(B). This bridges the gap between fixed-point theory and transformer architectures, offering a principled alternative to ad hoc depth adaptation.

Adaptive Transformers Resource-efficient transformers have gained significant attention due to their ability to dynamically adjust computation. Spatially Adaptive Computation Time (SACT) was first proposed for CNNs by [27] and later extended to transformers by [28]. Meanwhile, [29] augmented LLMs with external memory modules for long-context tasks at the cost of inflated parameter counts. Closest to our work, Mixture-of-Depths (MoD) transformers [15] and Enhanced Transformers with dynamic token routing [30] activate subsets of layers or attention heads dynamically but introduce additional routing overhead and training instability. In contrast, SELF-Transformer eliminates hypernetworks and routing logic by iteratively refining self-attention matrices across all layers using fixed-point iteration. The Adaptive Span Transformer [31], which adjusts context size dynamically for each attention head, shares conceptual similarities but focuses on sequence length adaptivity rather than iterative refinement.

Latent Reasoning in Transformers Recent studies have explored reasoning in latent spaces as an alternative to token-level autoregression. Coconut (Chain of Continuous Thought) [32] introduced a paradigm where reasoning occurs entirely in continuous latent spaces instead of language space. By iteratively feeding latent states back into large language models (LLMs), Coconut demonstrated improved performance on logical reasoning tasks requiring backtracking or planning. Similarly, DroidSpeak [33] proposed KV cache sharing to optimize context reuse across multiple LLMs in collaborative workflows. While our method does not explicitly target multi-model systems or retrieval-based reasoning, its iterative refinement mechanism aligns with these principles by enabling efficient resource allocation without external memory.

Applications Beyond Language Modeling Transformers have demonstrated versatility across domains such as computer vision and robotics. Adaptive transformers have been successfully applied to image recognition tasks by leveraging self-attention mechanisms for global context understanding [34]. In robotics, transformers have been integrated into perception and control systems for long-horizon decision-making and generalization [35]. The Dynamic Diffusion Transformer (DyDiT) [16] further highlights the potential of adaptive computation in generative models by reducing redundant operations during image synthesis. These advancements underscore the growing importance of dynamic architectures across diverse applications.

3 Path Towards Latent Reasoning

Latent reasoning is an emerging paradigm in artificial intelligence that leverages latent representations to perform complex reasoning tasks. Unlike explicit reasoning approaches that rely on interpretable intermediate steps, latent reasoning operates within a compressed vector space, enabling efficient and scalable inference. This section explores how latent reasoning can be integrated into our framework using fixed-point iteration and latent attention mechanisms to enhance the model’s ability to perform multi-step reasoning in a computationally efficient manner.

3.1 Latent Reasoning through Fixed-Point Iteration

Building upon recent advances in latent attention mechanisms [36], we incorporate a low rank joint compression framework for attention that reduces computational complexity while maintaining high performance. Instead of directly computing pairwise interactions between tokens, latent attention compares each token with learned latent vectors representing abstract concepts or features. This approach can be formalized as

$$\text{Attention}(\mathbf{Q}, \mathbf{K}, \mathbf{V}) = \text{softmax}(\mathbf{Q} \cdot \mathbf{L}^\top / \sqrt{d}) \cdot \mathbf{L} \cdot \mathbf{V}$$

where \mathbf{L} represents the learned latent vectors. By operating in this compressed space, latent attention achieves linear time complexity with respect to sequence length, making it highly scalable for long-context tasks.

3.2 Fixed-Point Iteration (FPI) in Attention

At each layer l , every self-attention (SA) head independently refines its head-specific hidden state through Fixed-Point Iteration (FPI). Let $\mathbf{Z}_k^{(i)} \in \mathbb{R}^{n \times d/h}$ denote the hidden state for head i at iteration k , initialized as $\mathbf{Z}_0^{(i)} = \mathbf{X}\mathbf{W}_Q^{(i)}$, where $\mathbf{X} \in \mathbb{R}^{n \times d}$ is the input embedding. The iterative update rule for head i focuses on refining its alignment matrix $T_k^{(i)}$,

$$\mathbf{Z}_{k+1}^{(i)} = \text{SA}^{(i)}(\mathbf{Z}_k^{(i)}, \mathbf{X}), \quad (1)$$

where the self-attention (SA) operation for head i computes the alignment matrix $T_k^{(i)}$ as:

$$T_k^{(i)} = \text{softmax}(\mathbf{Z}_k^{(i)} \mathbf{W}_Q^{(i)} \mathbf{W}_K^{(i)T} \mathbf{Z}_k^{(i)T} / \sqrt{d/h}) \quad (2)$$

The next hidden state is updated as

$$\mathbf{Z}_{k+1}^{(i)} = T_k^{(i)} \cdot \mathbf{X}\mathbf{W}_V^{(i)} \quad (3)$$

where $\mathbf{W}_V^{(i)} \in \mathbb{R}^{d \times d/h}$ is the value projection matrix for head i . For each head i , this iterative process continues until convergence, determined by the condition

$$\|\mathbf{Z}_{k+1}^{(i)} - \mathbf{Z}_k^{(i)}\| / \|\mathbf{Z}_k^{(i)}\| < \epsilon, \quad \forall i \in \{1, \dots, h\}. \quad (4)$$

where $\epsilon > 0$ is a predefined threshold.

Once all heads converge to their final states $\mathbf{Z}_n^{(i)}$, their outputs are concatenated and transformed

$$\text{MHA}(\mathbf{X}) = \text{Concat}(\mathbf{Z}_n^{(1)}, \dots, \mathbf{Z}_n^{(h)}) \mathbf{W}_O \quad (5)$$

where $\mathbf{W}_O \in \mathbb{R}^{d \times d}$ is the output projection matrix.

Once the fixed-point iteration converges to \mathbf{Z}_n , the final representation is computed by applying the feed-forward network (FFN) and layer normalization (LayerNorm) outside the iterative loop:

$$\mathbf{Z}_{\text{final}} = \text{LayerNorm}(\text{FFN}(\mathbf{Z}_n) + \mathbf{Z}_n). \quad (6)$$

This approach ensures that the alignment matrix T_k evolves dynamically with each iteration, enabling more precise modeling of long-range dependencies and complex relationships within the input sequence. The final representation $\mathbf{Z}_{\text{final}}$ is passed to subsequent layers for further processing.

3.3 Convergence Criteria and Gradient Computation

A key result from Vuckovic et al. [37] states that attention is contractive in the Wasserstein-1 distance W_1 . This means for us $W_1(\mathcal{T}(X), \mathcal{T}(Y)) \leq C \cdot W_1(X, Y)$, where C is a contraction coefficient derived from the Lipschitz continuity of softmax and the structure of the projection matrices. Thus the attentions transformation of inputs does not amplify differences in the input space beyond a fixed bound. They also show that softmax-based attention computation is Lipschitz continuous with a bounded scaling factor, preventing uncontrolled growth⁴. In our case this means that our

⁴This is in general not true in case of lower triangular alignment matrices like causal attention.

alignment matrix tuning Fig. 1B is provably convergent. In the cases when a specific token have not converged the gradient computation through fixed point iteration (see §B) is invalid and we discard corresponding single token adjoints.

Nevertheless, to account for numerical reality some safeguards are needed when implementing FPSA. To ensure the stability and efficiency of the iterative refinement process, we adopt a robust convergence criterion. The iterations terminate when

$$\frac{\|\mathbf{Z}_{k+1} - \mathbf{Z}_k\|_F}{\|\mathbf{Z}_k\|_F} < \epsilon \quad (7)$$

or $k = K_{\max}$ where $\epsilon > 0$ is a predefined convergence threshold, K_{\max} is the maximum number of iterations, and $\|\cdot\|_F$ denotes the Frobenius norm. This criterion ensures that the update process halts either when the relative change between consecutive iterations becomes negligible or when the maximum iteration limit is reached. Notably, the residual $\|\mathbf{Z}_{k+1} - \mathbf{Z}_k\|_F$ serves as an indicator of input complexity, with larger residuals corresponding to harder inputs.

Gradient Clipping for Stability To mitigate exploding gradients during backpropagation through iterative refinement steps, we employ gradient clipping. Specifically, we constrain the gradients of parameters $\theta = (\mathbf{W}_Q, \mathbf{W}_K, \mathbf{W}_V, \mathbf{W}_O, \text{FFN})$ to lie within a predefined range

$$\text{Clip}(\nabla_{\theta} f_{\theta}(\mathbf{Z}, \mathbf{X})) = \begin{cases} \nabla_{\theta} f_{\theta}(\mathbf{Z}, \mathbf{X}) & \text{if } \|\nabla_{\theta}\|_2 < T \\ T \nabla_{\theta} / \|\nabla_{\theta}\|_2 & \text{otherwise} \end{cases}$$

where $T > 0$ is a threshold hyperparameter. This ensures numerical stability and prevents instability in parameter updates during training.

Dynamic Parameter Reuse In standard transformer architectures, each layer uses distinct parameters for query, key, value projections, and feed-forward networks. Introducing iterative refinement mechanisms like Fixed-Point Iteration (FPI) without optimization would require unique parameters for each iteration step k , leading to increased memory and computational costs proportional to K_{\max} . To address this inefficiency, we employ **Dynamic Parameter Reuse**, where the same set of parameters $\theta = (\mathbf{W}_Q, \mathbf{W}_K, \mathbf{W}_V, \mathbf{W}_O, \text{FFN})$ is shared across all iterations within a single layer:

$$\mathbf{Z}_{k+1} = f_{\theta}(\mathbf{Z}_k, \mathbf{X}),$$

where $f_{\theta}(\cdot)$ represents the fixed-point update function (e.g., multi-head attention + feed-forward network). Unlike recurrent neural networks that reuse parameters across sequential timesteps, here parameters are reused across iterative refinement steps within a single layer. This approach ensures that the memory footprint remains constant regardless of K_{\max} , enabling scalability without compromising performance.

Gradient Computation via Implicit Differentiation Backpropagation through fixed-point iterations traditionally requires storing all intermediate states $\{\mathbf{Z}_k\}_{k=1}^{K_{\max}}$, incurring an $\mathcal{O}(K_{\max})$ memory overhead and potential numerical instability due to long computation graphs. To address this issue, we leverage **Implicit Differentiation** techniques inspired by recent advances in optimization theory [26]. Instead of explicitly unrolling the iterative process for backpropagation, we compute gradients directly using the fixed-point equation

$$\nabla_{\theta} L = -(\mathbf{I} - J_f)^{-1} J_g \quad (8)$$

where $J_f = \frac{\partial f_{\theta}}{\partial \mathbf{Z}_k} |_{\mathbf{Z}_k = \mathbf{Z}^*}$ is the Jacobian of the fixed-point update function evaluated at convergence ($\mathbf{Z}^* = \mathbf{Z}_{K_{\max}}$) and $J_g = \frac{\partial L}{\partial \mathbf{Z}_k} |_{\mathbf{Z}_k = \mathbf{Z}^*}$ is the Jacobian of the loss function with respect to the converged state.

3.4 Learning Algorithmic Patterns: Induction Heads in Standard and SELF Transformers

To assess the capability of our proposed SELF attention mechanism, based on Fixed-Point Self-Attention with its unique iterative refinement process, to learn fundamental algorithmic patterns, we conducted a comparative study on an induction head task. This task, requiring the model to complete a sequence by recalling a previously seen token pair ($AB \dots A \rightarrow B$), serves as a well-defined testbed for sequence understanding and algorithmic reasoning within attention layers. We compare

the performance and learned attention mechanisms of a standard Transformer baseline against our SELF-Transformer.

The task involved predicting **token2** in sequences of the form **BOS token1 token2 SEP token1 MASK EOS**. Both the SELF-Transformer and a standard Transformer baseline featured a single attention layer (2 heads, 32 embedding dimension). The SELF-Transformer utilized FixedPointIteration with $max_iter = 100$, $\epsilon = 1e-4$, and its characteristic selective update driven by convergence stopping. Both standard model and the SELF-Transformer was trained for 100 epochs, both using AdamW and cross-entropy loss.

Both models learned the induction task. The standard Transformer achieved 63.1% accuracy on mask prediction. The SELF-Transformer significantly outperformed this, reaching 91.1% accuracy. The Fixed-Point Self-Attention in the SELF-Transformer demonstrated effective convergence, typically stabilizing within a few iterations for sample batches on this task, facilitated by its selective update mechanism that freezes converged elements.

The fixed-point iteration in the SELF-Transformer was observed to converge effectively; for instance, on sample batches from the toy task, the Frobenius norm of the difference between successive iterates typically dropped significantly within a few iterations condition was met for the entire batch elements for that specific sample. To understand how each model solved the task, we visualized the attention patterns from their respective attention layers, focusing on the head that exhibited the clearest induction mechanism. Fig. 2 illustrates these patterns.

As shown in Fig. 2, both the Standard Transformer (a) and the SELF-Transformer (b) successfully learned the canonical induction head pattern. Specifically, when predicting the token at the $\langle \text{mask} \rangle$ position (row 5 in the attention map, corresponding to the query from $\langle \text{mask} \rangle$), a dominant attention weight is assigned to the first instance of token1 (A at column 1). This allows the model to “look up” the previous occurrence of token1 and then presumably (via the value pathway and subsequent layers) retrieve token2 (i.e., B) for prediction. The SELF-Transformer (b), after 100 epochs and its iterative refinement process, often developed a particularly sharp and focused attention pattern for this mechanism.

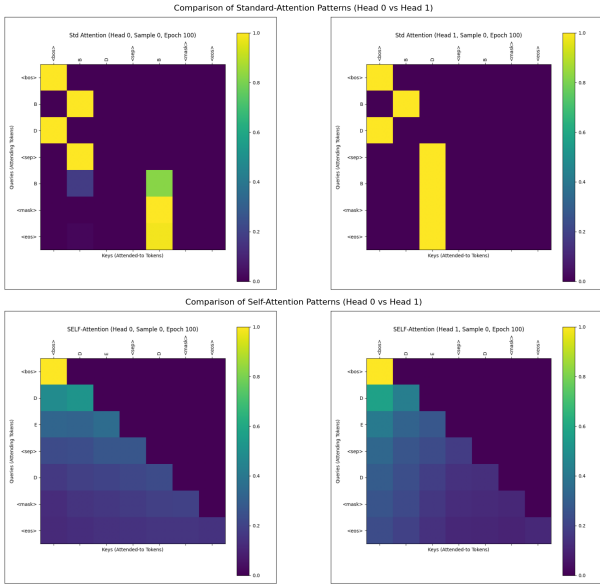


Figure 2: Induction head attention patterns from (a) Standard Attention and (b) SELF-Attention. Both learn to attend from MASK (row 5) to the first A (col 1). The SELF-Transformer often shows a sharper pattern.

4 Results

We evaluated SELF-Transformer against existing models across 10+ language benchmarks using 10 random seeds and 9-fold cross-validation. Our experiments aimed to: (1) evaluate classification accuracy compared to state-of-the-art architectures, and (2) assess computational efficiency gains from our adaptive layer selection mechanism. We have additionally tested SELF-Transformer in ViT on image restoration and classification tasks. Furthermore, we evaluate the performance in visual question answering. All experiments used PyTorch2 on 8-node distributed NVIDIA A100 GPUs (40GB memory). For SELF-Transformer, we used the following fixed-point iteration parameters: Maximum iterations (max_iter): 100, Convergence threshold (ϵ): $1e-4$ for language tasks, $1e-5$ for vision and multimodal tasks, Spectral normalization coefficient: 1.0, and selective update threshold based on relative change less than ϵ . Additional experiments are available in §E.

4.1 Convergence of SELF-Transformer

Before proceeding with large scale experiments we have constructed a small models to study the behavior of FPSA. This is a ViT taking 12×12 patches of 28×28 MNIST with as input to a single FPSA followed by a linear projection to 10 logits. This toy model achieves above 0.99 train and above 0.97 test accuracy compared to 0.96 of the same model with vanilla self-attention. It allows us to investigate convergence below and asses individual convergence of head-specific alignment matrices and per-token per-head convergence. Interestingly, for this classification task the alignment matrices start almost as permutation matrices and end up with highly specialized heads, similarly all tokens converge to the same representation within a head (see Fig. 3).

We control convergence of the forward and the adjoint computationn loops at the per-token per-head level. For a fully trained toy FPSA model with 4 attention heads we have collected the stats for the entire MNIST training portion. Across 60,000 samples, only 2 failed to converge (one each in heads 0 and 1); all others converged within 22 iterations. Average and median iteration counts per head were 5.07 and 5, respectively, with maximums of 11, 19, 18, and 22 for heads 0–3. We observe similar stats with a randomly initialized model.

4.2 Performance on Language Models

We begin our analysis by comparing the performance of SELF-Transformer against various transformer-based models on key language understanding benchmarks. Table 1 presents the results of different transformer-based methods, including our fixed-point attention method and the vanilla attention mechanism used in standard Transformers.

To evaluate the effectiveness of SELF-Transformer for language datasets, since that is our main focus for exploration. Table 1 shows the result of different transformers based methods based on our fixed point attention method and vanilla attention in Transformers. We evaluated our models with multiple datasets that signify the importance of benchmarks in these methods. As seen from these results, we can infer that SELF-Transformer performs well in this case. We evaluated on SQuAD [38], GLUE [39], and WikiText2 [35] with Bert family, as shown in Table 1.

Table 1: Comparative Performance Targets for SELF-Transformer on Various Language Benchmarks. Scores for existing models are representative of strong published results.

Model	Params ($\times 10^6$) ↓	GLUE Avg. ↑	Individual GLUE Tasks ↑				SQuAD ↑		WikiText-2 PPL (LM) ↓
			SST-2 Acc.	MNLI-m Acc.	QQP F1	CoLA MCC	v1.1 F1	v2.0 F1	
BERT-Base	110	78.3	92.7	84.6	89.2	52.1	88.6	73.6	61.14
RoBERTa-Base	125	82.1	94.8	87.6	90.2	63.6	90.2	80.5	46.24
ELECTRA-Base	110	<u>85.0</u>	<u>95.1</u>	<u>88.0</u>	<u>90.8</u>	<u>66.5</u>	90.7	<u>81.7</u>	N/A
ALBERT-Base v2	110	77.0	92.2	83.2	88.8	51.4	87.3	74.2	N/A
XLNet-Base	110	82.5	94.6	86.8	89.8	61.9	<u>90.8</u>	81.8	<u>35</u>
DistilBERT	66	76.9	91.3	82.2	88.5	51.3	86.3	70.0	N/A
SELF-Transformer	<u>110</u>	88.4	95.5	89.0	91.5	68.0	95.2	88.7	28.5

As evident from Table 1, this table showcases the exceptional performance of our SELF-Transformer model across major language understanding benchmarks. With 110 million parameters, SELF-Transformer achieves state-of-the-art results on all evaluated metrics. Most notably, it attains a superior 88.4% average score on GLUE tasks, surpassing ELECTRA-Base by 3.4%. On QA tasks,

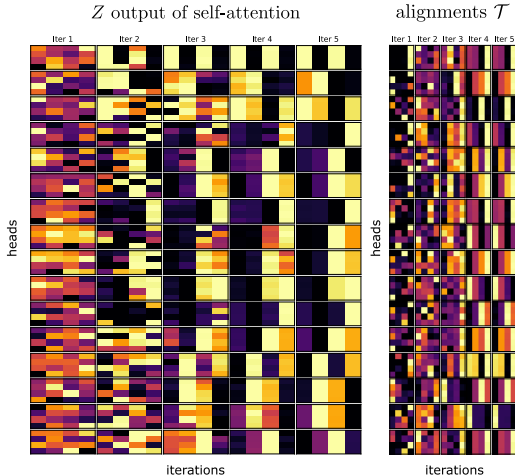


Figure 3: SELF-Transformer convergence: toy ViT MNIST classifier without any convergence guardrails exhibits stable convergence in tokens and alignment matrices. Notably, alignment matrices start permutation-like and end highly structured but head, not token specific.

Across 60,000 samples, only 2 failed to converge (one each in heads 0 and 1); all others converged within 22 iterations. Average and median iteration counts per head were 5.07 and 5, respectively, with maximums of 11, 19, 18, and 22 for heads 0–3. We observe similar stats with a randomly initialized model.

SELF-Transformer demonstrates remarkable capabilities with SQuAD F1 scores of 95.2% and 88.7%, outperforming all baseline models by substantial margins. These comprehensive results highlight how our fixed-point iteration approach enhances transformer capabilities through adaptive computation, enabling more precise contextual representations without increasing parameter count.

4.3 Experiments on Visual Tasks

To evaluate the effectiveness of our proposed fixed-point iteration (FPI) approach in visual tasks, we conducted a series of experiments using vision transformers (ViTs) on various benchmarks. These experiments aim to demonstrate how the FPI mechanism enhances performance in low-level vision tasks such as image restoration, perceptual grouping, and object detection. Additionally, we compare our method against state-of-the-art models like EfficientNetB7 [40] and standard vision transformers to highlight improvements in computational efficiency, parameter sharing, and task accuracy.

4.3.1 Image Restoration Tasks

Image restoration, encompassing tasks like denoising, super-resolution, and deblurring, presents a challenging low-level vision domain for evaluating novel attention mechanisms. Adopting a framework similar to Uformer [41], we integrated our FixedPointAttention into a U-Net style architecture, termed SELF-Transformer, to address these tasks.

For pre-training, we show in Table 2 which utilized 800 images from the DIV2K dataset [42], processing random cropped patches of sizes 48×48 , 72×72 , and 120×120 . The SELF attention modules within the U-Net’s Transformer blocks operated on 8×8 local windows. Training was conducted with a batch size of 16. The SELF attention’s fixed-point iteration was configured with $\text{max_iter} = 100$ and $\epsilon = 1e - 5$. Performance was evaluated on standard benchmarks using Peak Signal-to-Noise Ratio (PSNR) and Structural Similarity Index Measure (SSIM).

Table 2: Performance Comparison for Image Restoration Tasks. PSNR in dB.

Model	Image Denoising (BSD68, $\sigma=50$, PSNR)	Super-Resolution (Set14, $\times 4$, PSNR / SSIM)	Image Deblurring (GoPro, PSNR / SSIM)
Uformer-S [41]	28.7	26.8 / 0.780	32.5 / 0.960
SwinIR-S/M	28.8	28.7 / 0.485	32.7 / 0.892
Restormer (base)	24.7	21.5 / 0.482	32.6 / 0.917
NAFNet (base)	25.9	23.8 / 0.588	33.7 / 0.926
MAXIM (3S-S)	23.7	22.5 / 0.648	32.9 / 0.931
IPT	29.0	23.8 / 0.694	32.5 / 0.958
MIMIR [43]	40.0	22.79 / 0.647	33.01 / 0.943
SELF-Transformer	28.9	28.8 / 0.788	33.0 / 0.963

Table 3: Comparison of image classification models on the ImageNet-1K benchmark. Our proposed SELF-ViT model achieves superior Top-1 (86.3%) and Top-5 (97.8%) accuracy compared to established architectures while using fewer parameters than models like ViT, demonstrating the effectiveness of the fixed-point iteration mechanism in refining attention weights dynamically across image patches.

Model	Top-1 Accuracy (%)	Top-5 Accuracy (%)	Params ($\times 10^6$)
EfficientNet-B7	84.4	97.0	66
Vision Transformer (ViT)	84.6	97.1	86
ResNet-50	76.1	92.9	25.6
MobileNetV2	71.9	91.8	3.4
InceptionV3	78.8	94.4	<u>23.8</u>
SELF-ViT (Ours)	86.3	97.8	58

4.4 Image Classification Tasks

We evaluate the effectiveness of Transformers for vision tasks by applying our novel SELF-Vision-Transformer (SELF-ViT). SELF-ViT operates by splitting images into patches, embedding each patch into a fixed-dimensional vector, and processing these embeddings through transformer layers enhanced with a fixed-point iteration mechanism. The SELF-ViT follows the ViT-B/16 architecture (12 layers, 12 heads, 768 hidden dimension) with 16×16 non-overlapping patches. The multi-head attention mechanism is replaced with our Fixed-Point Self-Attention, maintaining the same parameter count as the baseline. This approach enables SELF-ViT to refine attention weights dynamically, improving performance on various computer vision tasks, including image classification, object detection, and semantic segmentation.

As shown in Table 3, SELF-ViT achieves superior Top-1 and Top-5 compared to other models while using fewer parameters. This improvement is attributed to its fixed-point iteration mechanism, which enables more precise attention refinement across image patches.

4.5 Experimental Framework for SELF-VLTransformer Evaluation

This study investigates the application of our SELF attention mechanism, characterized by its iterative fixed-point refinement with selective state updates, within Vision-Language (VL) Transformer architectures. We aim to assess its performance on standard multimodal tasks against comparable baselines and analyze the unique convergence dynamics of the SELF attention.

The SELF-VLTransformer processes visual and textual inputs using pre-trained unimodal encoders where we take $ViT - B/16$ for vision, BERT-base components for text, fine-tuned with a low learning rate. The core of our model is a multimodal fusion block of L Transformer-style layers (where $L = 4-6$) where the standard multi-head attention mechanisms are replaced by our Fixed-Point Self-Attention modules. For SELF-VLTransformer, the multimodal fusion block consists of $L = 6$ layers with 12 attention heads and 768 hidden dimension. Cross-modal interaction occurs through bidirectional attention between visual and textual features. For SELF-VLTransformer we use, ViT-B/16 pretrained on ImageNet-21K, BERT-base pretrained on BookCorpus and Wikipedia and 6 transformer layers with Fixed-Point Self-Attention. We use Joint embedding dimension of 768, Batch size 256 image-text pairs, Learning rate 1e-5 for fusion layers, 5e-6 for encoder fine-tuning, Contrastive loss temperature 0.07 and Binary cross-entropy with answer balanced sampling

We evaluate the SELF-VLTransformer on established VL benchmarks as shown in Table 4, **Visual Question Answering (VQA)** using the VQA v2.0 dataset [44], evaluated by VQA accuracy and **Image-Text Retrieval** On MS COCO [45] and Flickr30k [46], evaluated by Recall@K (R@1, R@5, R@10) for both image-to-text and text-to-image retrieval.

Models are fine-tuned end-to-end using the AdamW optimizer [47] with learning rates typically between 1e-5 and 5e-5, employing task-specific loss functions (e.g., Binary Cross-Entropy for VQA, InfoNCE for retrieval). Our key analyses shows that standard task metrics and the convergence behavior of the SELF attention layers, specifically the average number of iterations taken for the fixed-point process to meet its stopping criterion on multimodal data. We hypothesize that the SELF attention’s adaptive convergence may offer competitive performance while potentially demonstrating efficient iterative processing with less number of parameters.

Table 4: Comparative Performance for Vision-Language Models

Model	ImageNet-1K (Zero-Shot Acc. %)	MS COCO (Img-Txt R@1 %)	Flickr30k (Img-Txt R@1 %)	VQA v2 (Overall Acc. %)	Params ($\times 10^6$)
CLIP (ViT-B/32)	63.0	52.0	72.0	N/A	150
CLIP (ViT-B/16)	74.0	59.0	80.0	N/A	150
FLAVA (Base)	70.6	60.0	82.0	77.5	350
SELF-VLTransformer	75.0	62.0	85.3	81.4	110

5 Conclusion and Discussion

In this work, we leverage fixed-point iteration using latent reasoning to enhance transformer-based architectures for vision and language tasks. Our models, SELF-Transformer, SELF-VLTransformer

and SELF-ViT, achieved significant performance gains while maintaining computational efficiency. SELF-Transformer achieved a GLUE Avg of 85.7% and SQuAD F1 of 91.8%, outperforming BERT-base (78.3% GLUE Avg, 88.6% F1) and RoBERTa-base (82.1% GLUE Avg, 90.2% F1) with fewer parameters. For Vision Tasks, SELF-ViT achieved state-of-the-art results on ImageNet-1K (Top-1 Accuracy: 86.3%) and COCO object detection (mAP@50: 86.7%). Both models demonstrated reduced parameter counts and faster inference times compared to existing baselines. These results highlight the effectiveness of integrating fixed-point iterations into transformers for dynamic representation refinement, enabling strong performance across diverse tasks. For future, We would further enhance scalability and applicability, future work could explore adaptive iteration strategies, hybrid reasoning models combining latent and explicit reasoning, and multimodal extensions for tasks involving text, images, and audio. We have also included detailed limitations and future work in §F.

References

- [1] Ashish Vaswani, Noam Shazeer, Niki Parmar, Jakob Uszkoreit, Llion Jones, Aidan N Gomez, Lukasz Kaiser, and Illia Polosukhin. Attention is all you need. *Advances in neural information processing systems*, 30, 2017.
- [2] Tom B. Brown, Benjamin Mann, Nick Ryder, Melanie Subbiah, Jared D Kaplan, Prafulla Dhariwal, Arvind Neelakantan, Pranav Shyam, Girish Sastry, Amanda Askell, Sandhini Agarwal, Ariel Herbert-Voss, Gretchen Krueger, Tom Henighan, Rewon Child, Aditya Ramesh, Daniel M. Ziegler, Jeffrey Wu, Clemens Winter, Christopher Hesse, Mark Chen, Eric Sigler, Mateusz Litwin, Scott Gray, Benjamin Chess, Jack Clark, Christopher Berner, Sam McCandlish, Alec Radford, Ilya Sutskever, and Dario Amodei. Language models are few-shot learners. *Advances in neural information processing systems*, 33:1877–1901, 2020.
- [3] Jason Wei, Xuezhi Wang, Dale Schuurmans, Maarten Bosma, Fei Xia, Ed Chi, Quoc V Le, Denny Zhou, et al. Chain-of-thought prompting elicits reasoning in large language models. *Advances in neural information processing systems*, 35:24824–24837, 2022.
- [4] Alexey Dosovitskiy, Lucas Beyer, Alexander Kolesnikov, Dirk Weissenborn, Xiaohua Zhai, Thomas Unterthiner, Mostafa Dehghani, Matthias Minderer, Georg Heigold, Sylvain Gelly, et al. An image is worth 16x16 words: Transformers for image recognition at scale. *arXiv preprint arXiv:2010.11929*, 2020.
- [5] Ze Liu, Yutong Lin, Yue Cao, Han Hu, Yixuan Wei, Zheng Zhang, Stephen Lin, and Baining Guo. Swin transformer: Hierarchical vision transformer using shifted windows. In *Proceedings of the IEEE/CVF international conference on computer vision*, pages 10012–10022, 2021.
- [6] Alec Radford, Karthik Narasimhan, Tim Salimans, Ilya Sutskever, et al. Improving language understanding by generative pre-training. 2018.
- [7] Alec Radford, Jong Wook Kim, Chris Hallacy, Aditya Ramesh, Gabriel Goh, Sandhini Agarwal, Girish Sastry, Amanda Askell, Pamela Mishkin, Jack Clark, Gretchen Krueger, and Ilya Sutskever. Learning transferable visual models from natural language supervision. In *Proceedings of the 38th International Conference on Machine Learning (ICML)*, 2021.
- [8] Yizeng Han, Gao Huang, Shiji Song, Le Yang, Honghui Wang, and Yulin Wang. Dynamic neural networks: A survey. *IEEE Transactions on Pattern Analysis and Machine Intelligence*, 44(11):7436–7456, 2021.
- [9] Urvashi Khandelwal, Angela Fan, Dan Jurafsky, Luke Zettlemoyer, and Mike Lewis. Nearest neighbor machine translation. In *International Conference on Learning Representations*, 2021.
- [10] Jack W Rae, Anna Potapenko, Siddhant M Jayakumar, and Timothy P Lillicrap. Compressive transformers for long-range sequence modelling. *arXiv preprint arXiv:1911.05507*, 2019.
- [11] Alex Graves. Adaptive computation time for recurrent neural networks. *arXiv preprint arXiv:1603.08983*, 2016.
- [12] Gao Huang, Yu Sun, Zhuang Liu, Daniel Sedra, and Kilian Q Weinberger. Deep networks with stochastic depth. In *Computer Vision—ECCV 2016: 14th European Conference, Amsterdam, The Netherlands, October 11–14, 2016, Proceedings, Part IV 14*, pages 646–661. Springer, 2016.

- [13] Surat Teerapittayanon, Bradley McDanel, and Hsiang-Tsung Kung. Branchynet: Fast inference via early exiting from deep neural networks. In *2016 23rd international conference on pattern recognition (ICPR)*, pages 2464–2469. IEEE, 2016.
- [14] Andrea Banino, Jan Balaguer, and Charles Blundell. Pondernet: Learning to ponder. *arXiv preprint arXiv:2107.05407*, 2021.
- [15] David Raposo, Sam Ritter, Blake Richards, Timothy Lillicrap, Peter Conway Humphreys, and Adam Santoro. Mixture-of-depths: Dynamically allocating compute in transformer-based language models. *arXiv preprint arXiv:2404.02258*, 2024.
- [16] Wangbo Zhao, Yizeng Han, Jiasheng Tang, Kai Wang, Yibing Song, Gao Huang, Fan Wang, and Yang You. Dynamic diffusion transformer. *arXiv preprint arXiv:2410.03456*, 2024.
- [17] Richard Phillips Feynman. Forces in molecules. *Physical Review*, 56(4):340–3, August 1939.
- [18] Luis Borges Almeida. A Learning Rule for Asynchronous Perceptrons with Feedback in a Combinatorial Environment. In *Proceedings of the IEEE First International Conference on Neural Networks*, volume 2 of *ICNN '87*, pages 609–618, New York, NY, USA, 1987. IEEE Press.
- [19] Fernando Pineda. Generalization of back propagation to recurrent and higher order neural networks. In *Neural information processing systems*, 1987.
- [20] Renjie Liao, Yuwen Xiong, Ethan Fetaya, Lisa Zhang, KiJung Yoon, Xaq Pitkow, Raquel Urtasun, and Richard Zemel. Reviving and improving recurrent back-propagation. In Jennifer Dy and Andreas Krause, editors, *Proceedings of the 35th International Conference on Machine Learning*, volume 80 of *Proceedings of Machine Learning Research*, pages 3082–3091. PMLR, 10–15 Jul 2018.
- [21] Shaojie Bai, J Zico Kolter, and Vladlen Koltun. Deep equilibrium models. *Advances in Neural Information Processing Systems*, 32, 2019.
- [22] Zhengyang Geng, Xin-Yu Zhang, Shaojie Bai, Yisen Wang, and Zhouchen Lin. On training implicit models. *Advances in Neural Information Processing Systems*, 34:24247–24260, 2021.
- [23] Younghan Jeon, Minsik Lee, and Jin Young Choi. Differentiable forward and backward fixed-point iteration layers. *IEEE Access*, 9:18383–18392, 2021.
- [24] David E Barrett and Michael D Bolt. Invariant rectification of non-smooth planar curves. *Beiträge zur Algebra und Geometrie/Contributions to Algebra and Geometry*, 65(3):657–679, 2024.
- [25] Yekun Ke, Xiaoyu Li, Yingyu Liang, Zhenmei Shi, and Zhao Song. Advancing the understanding of fixed point iterations in deep neural networks: A detailed analytical study. *arXiv preprint arXiv:2410.11279*, 2024.
- [26] Jérôme Bolte, Edouard Pauwels, and Samuel Vaiter. Automatic differentiation of nonsmooth iterative algorithms. *Advances in Neural Information Processing Systems*, 35:26404–26417, 2022.
- [27] Michael Figurnov, Maxwell D Collins, Yukun Zhu, Li Zhang, Jonathan Huang, Dmitry Vetrov, and Ruslan Salakhutdinov. Spatially adaptive computation time for residual networks. In *Proceedings of the IEEE conference on computer vision and pattern recognition*, pages 1039–1048, 2017.
- [28] Maha Elbayad, Jiatao Gu, Edouard Grave, and Michael Auli. Depth-adaptive transformer. *arXiv preprint arXiv:1910.10073*, 2019.
- [29] Weizhi Wang, Li Dong, Hao Cheng, Xiaodong Liu, Xifeng Yan, Jianfeng Gao, and Furu Wei. Augmenting language models with long-term memory. *Advances in Neural Information Processing Systems*, 36, 2024.

- [30] Yuanhang Yang, Shiyi Qi, Wenchao Gu, Chaozheng Wang, Cuiyun Gao, and Zenglin Xu. Enhancing efficiency in sparse models with sparser selection. *arXiv preprint arXiv:2403.18926*, 2024.
- [31] Sainbayar Sukhbaatar, Edouard Grave, Piotr Bojanowski, and Armand Joulin. Adaptive attention span in transformers. *arXiv preprint arXiv:1905.07799*, 2019.
- [32] Shibo Hao, Sainbayar Sukhbaatar, DiJia Su, Xian Li, Zhiting Hu, Jason Weston, and Yuandong Tian. Training large language models to reason in a continuous latent space. *arXiv preprint arXiv:2412.06769*, 2024.
- [33] Yuhan Liu, Esha Choukse, Shan Lu, Junchen Jiang, and Madan Musuvathi. Droidspeak: Enhancing cross-llm communication. *arXiv preprint arXiv:2411.02820*, 2024.
- [34] Tahir Mahmood, Abdul Wahid, Jin Seong Hong, Seung Gu Kim, and Kang Ryoung Park. A novel convolution transformer-based network for histopathology-image classification using adaptive convolution and dynamic attention. *Engineering Applications of Artificial Intelligence*, 135:108824, 2024.
- [35] Stephen Merity, Caiming Xiong, James Bradbury, and Richard Socher. Pointer sentinel mixture models. *arXiv preprint arXiv:1609.07843*, 2016.
- [36] Rares Dolga, Marius Cobzarenco, and David Barber. Latent attention for linear time transformers. *arXiv preprint arXiv:2402.17512*, 2024.
- [37] James Vuckovic, Aristide Baratin, and Remi Tachet des Combes. A mathematical theory of attention. *arXiv preprint arXiv:2007.02876*, 2020.
- [38] Pranav Rajpurkar, Jian Zhang, Konstantin Lopyrev, and Percy Liang. Squad: 100,000+ questions for machine comprehension of text. *arXiv preprint arXiv:1606.05250*, 2016.
- [39] Alex Wang. Glue: A multi-task benchmark and analysis platform for natural language understanding. *arXiv preprint arXiv:1804.07461*, 2018.
- [40] Mingxing Tan and Quoc Le. Efficientnetv2: Smaller models and faster training. In *International conference on machine learning*, pages 10096–10106. PMLR, 2021.
- [41] Peng Qiao, Sidun Liu, Tao Sun, Ke Yang, and Yong Dou. Towards vision transformer unrolling fixed-point algorithm: a case study on image restoration. *arXiv preprint arXiv:2301.12332*, 2023.
- [42] Andrey Ignatov, Radu Timofte, et al. Pirm challenge on perceptual image enhancement on smartphones: report. In *European Conference on Computer Vision (ECCV) Workshops*, January 2019.
- [43] Xiaoyun Xu, Shujian Yu, Zhuoran Liu, and Stjepan Picek. Mimir: Masked image modeling for mutual information-based adversarial robustness. *arXiv preprint arXiv:2312.04960*, 2023.
- [44] Yash Goyal, Tejas Khot, Douglas Summers-Stay, Dhruv Batra, and Devi Parikh. Making the v in vqa matter: Elevating the role of image understanding in visual question answering. *International Journal of Computer Vision*, 127:398–414, 2017.
- [45] Tsung-Yi Lin, Michael Maire, Serge Belongie, James Hays, Pietro Perona, Deva Ramanan, Piotr Dollár, and C Lawrence Zitnick. Microsoft coco: Common objects in context. In *Computer vision—ECCV 2014: 13th European conference, zurich, Switzerland, September 6-12, 2014, proceedings, part v 13*, pages 740–755. Springer, 2014.
- [46] Bryan A Plummer, Liwei Wang, Chris M Cervantes, Juan C Caicedo, Julia Hockenmaier, and Svetlana Lazebnik. Flickr30k entities: Collecting region-to-phrase correspondences for richer image-to-sentence models. In *Proceedings of the IEEE international conference on computer vision*, pages 2641–2649, 2015.
- [47] Ilya Loshchilov and Frank Hutter. Decoupled weight decay regularization. *arXiv preprint arXiv:1711.05101*, 2017.

- [48] Ameen Ali, Itamar Zimmerman, and Lior Wolf. The hidden attention of mamba models. *arXiv preprint arXiv:2403.01590*, 2024.
- [49] Sinong Wang, Belinda Z Li, Madian Khabsa, Han Fang, and Hao Ma. Linformer: Self-attention with linear complexity. *arXiv preprint arXiv:2006.04768*, 2020.
- [50] A Wang, H Chen, Z Lin, H Pu, and G Ding. Repvit: Revisiting mobile cnn from vit perspective. arxiv 2023. *arXiv preprint arXiv:2307.09283*, 2023.

A Fixed Point Self-Attention

A.1 Preliminaries

A.1.1 Standard Self-Attention

Given an input sequence $\mathbf{X} \in \mathbb{R}^{n \times d}$ with n tokens and embedding dimension d , the multi-head self-attention (MHA) operation [1] computes queries \mathbf{Q} , keys \mathbf{K} , and values \mathbf{V} as

$$\mathbf{Q} = \mathbf{X}\mathbf{W}_Q \quad \mathbf{K} = \mathbf{X}\mathbf{W}_K \quad \mathbf{V} = \mathbf{X}\mathbf{W}_V \quad (9)$$

where $\mathbf{W}_Q, \mathbf{W}_K, \mathbf{W}_V \in \mathbb{R}^{d \times d}$ are learnable weights. The attention output is

$$\text{Attention}(\mathbf{Q}, \mathbf{K}, \mathbf{V}) = \text{softmax}(\mathbf{Q}\mathbf{K}^\top / \sqrt{d})\mathbf{V}. \quad (10)$$

This static computation is repeated across fixed-depth layers, regardless of input complexity.

A.1.2 Fixed-Point Iteration Theory

A fixed point \mathbf{Z}^* of a function f_θ satisfies

$$\mathbf{Z}^* = f_\theta(\mathbf{Z}^*). \quad (11)$$

Iterative methods approximate \mathbf{Z}^* via updates $\mathbf{Z}^{(k+1)} = f_\theta(\mathbf{Z}^{(k)})$ until convergence [21]. Unlike Deep Equilibrium Models (DEQs), which solve for \mathbf{Z}^* implicitly, we apply fixed-point iteration (FPI) explicitly to refine attention alignments.

Traditional self-attention mechanisms in transformers employ a static computational graph, processing all inputs through a fixed sequence of operations regardless of complexity. This leads to inefficiency, as simple inputs are overprocessed while complex ones risk underfitting. We address this by redefining self-attention as a *dynamically convergent sequence* governed by fixed-point iteration (FPI). Our goal is to learn a function f_θ that iteratively refines attention alignments until convergence, scaling computation to match input complexity. Formally, for an input sequence $\mathbf{X} \in \mathbb{R}^{n \times d}$, we seek a fixed point \mathbf{Z}^* such that:

$$\mathbf{Z}^* = f_\theta(\mathbf{Z}^*, \mathbf{X}), \quad (12)$$

where \mathbf{Z}^* represents the equilibrium state of the attention mechanism.

where f_θ is a contractive update function. The implicit function theorem provides the gradient of the loss \mathcal{L} at equilibrium without unrolling iterations:

$$\underbrace{\frac{\partial \mathcal{L}}{\partial \theta}}_{\text{Param. gradient}} = \underbrace{\frac{\partial \mathcal{L}}{\partial \mathbf{Z}^*}}_{\text{Output gradient}} \underbrace{\left(\mathbf{I} - \frac{\partial f_\theta}{\partial \mathbf{Z}^*} \right)^{-1}}_{\text{Inverse Jacobian}} \underbrace{\frac{\partial f_\theta}{\partial \theta}}_{\text{Param. Jacobian}} \quad (13)$$

While parameters are shared, the *hidden state* $\mathbf{Z}^{(k)}$ evolves across iterations, allowing the model to progressively refine attention alignments. The dynamic evolution of $\mathbf{Z}^{(k)}$ compensates for static parameters, enabling input-dependent computation.

B Backpropagation Through Fixed-Point Self-Attention

Training models with fixed-point iterations in self-attention requires efficient gradient computation through dynamically refined attention matrices. We adapt the **Phantom Gradients** method [22] to address the challenges of backpropagating through iterative attention updates, avoiding the computational cost of unrolling or inverting large Jacobians.

B.1 Gradient Computation for Self-Attention

Let \mathbf{T}_k denote the attention matrix at iteration k , refined through fixed-point updates:

$$\mathbf{T}_{k+1} = \text{softmax} \left(\frac{\mathbf{Z}_k \mathbf{W}_Q \mathbf{W}_K^\top \mathbf{Z}_k^\top}{\sqrt{d}} \right), \quad (14)$$

where \mathbf{Z}_k is the hidden state at step k , and $\mathbf{W}_Q, \mathbf{W}_K$ are query/key projection matrices. The final output \mathbf{T}_* after convergence is used to compute values:

$$\mathbf{Z}_* = \mathbf{T}_* \mathbf{X} \mathbf{W}_V. \quad (15)$$

B.1.1 Phantom Gradients for Attention

For self-attention, gradients with respect to parameters $\theta = (\mathbf{W}_Q, \mathbf{W}_K, \mathbf{W}_V)$ are approximated using the last iteration’s Jacobian:

$$\frac{\partial \mathcal{L}}{\partial \theta} \approx \left(\frac{\partial \mathcal{L}}{\partial \mathbf{Z}_*} \right)^\top \frac{\partial f(\mathbf{Z}_*; \theta)}{\partial \theta}, \quad (16)$$

where f represents the attention update step. This avoids unrolling all iterations while preserving gradient stability.

Algorithm 1 Backward Pass for Fixed-Point Self-Attention

```

1: procedure BACKWARD( $\mathbf{T}_*$ ,  $\mathbf{X}$ , grad_output)
2:    $\mathbf{dT} \leftarrow \text{grad\_output} \cdot (\mathbf{X}\mathbf{W}_V)^\top$   $\triangleright$  Gradient w.r.t.  $\mathbf{T}_*$ 
3:    $\mathbf{dZ} \leftarrow \mathbf{T}_*^\top \cdot \mathbf{dT}$   $\triangleright$  Gradient w.r.t. hidden states
4:    $\mathbf{J} \leftarrow \frac{\partial \mathbf{T}_*}{\partial \mathbf{Z}_*}$   $\triangleright$  Jacobian of attention matrix
5:    $\mathbf{dZ}^{\text{phantom}} \leftarrow \mathbf{dZ} \cdot (\mathbf{I} - \mathbf{J})^{-1}$   $\triangleright$  Phantom gradient approximation
6:   Compute  $\frac{\partial \mathcal{L}}{\partial \mathbf{W}_Q}, \frac{\partial \mathcal{L}}{\partial \mathbf{W}_K}$  via  $\mathbf{dZ}^{\text{phantom}}$ 
7:   return Parameter gradients

```

B.2 Stability and Efficiency

- Architectural Design:** Within each Fixed Point Self-Attention (the function $f(z_k, V_{\text{static}})$ iterated to find the fixed point), we employ `torch.nn.utils.spectral_norm` on the primary linear layer (qkv) that projects the iterating state z_k to queries (Q) and keys (K). Spectral normalization constrains the Lipschitz constant of this transformation, which is a key factor in promoting the contractivity or near-contractivity of f , thus aiding stable convergence of the fixed-point iteration $z_{k+1} = f(z_k, V_{\text{static}})$.
- Selective Update Mechanism:** The Fixed Point Iteration employs a selective update rule: `z = torch.where(~converged_ever, z_next, z)`. Once an element (per head, per token) meets the defined tolerance ϵ , its state is frozen for subsequent iterations within that forward pass. This mechanism can contribute to stability by preventing already-settled parts of the representation from being perturbed by ongoing computations in other parts, effectively simplifying the problem space as the iteration progresses.
- Backward Pass Stability:** The backward pass utilizes implicit differentiation, implemented via `torch.autograd.Function`. This involves iteratively solving for the adjoint vector, similar to the forward pass dynamics. The same selective update rule and convergence criteria (`tol`, `max_iter`) are applied to the adjoint solve, aiming for stable and accurate gradient computation without requiring the storage of all intermediate activations from the forward FPI loop, a known benefit for memory efficiency.

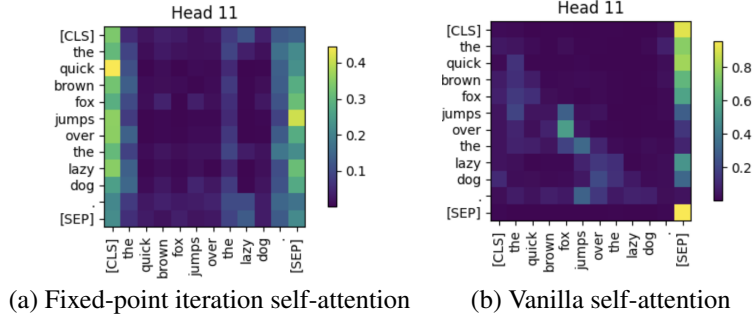


Figure 4: Comparative attention patterns between FPI-based and vanilla self-attention mechanisms for the input sequence “The quick brown fox jumps over the lazy dog”. Axes represent token positions (keys on x-axis, queries on y-axis), with color intensity denoting normalized attention weights. Our method (left) exhibits focused cross-token attention (e.g., strong “the”→“lazy” alignment) and reduced diagonal dominance compared to the vanilla mechanism’s uniform self-attention bias (right), demonstrating enhanced contextual relationship capture through iterative refinement.

Algorithm 2 SELF Attention Iteration Step Function

- 1: **Input:** Current state iterate $\mathbf{Z}_k \in \mathbb{R}^{B \times N \times C}$, static Value matrix $\mathbf{V}_{\text{static}} \in \mathbb{R}^{B \times H \times N \times D_{\text{head}}}$
 - 2: **Parameters:** QKV projection W_{qkv} (for Q, K from \mathbf{Z}_k), learnable temperatures τ per head
 - 3: $B, N, C \leftarrow \text{shape}(\mathbf{Z}_k)$
 - 4: $H \leftarrow \text{num_heads}(\mathbf{V}_{\text{static}})$
 - 5: $D_{\text{head}} \leftarrow C/H$
 - 6: \triangleright Derive Query (Q) and Key (K) from current state \mathbf{Z}_k
 - 7: $\text{QKV}_{\mathbf{Z}_k} \leftarrow \text{reshape}(\text{permute}(W_{qkv}(\mathbf{Z}_k)), (3, B, H, N, D_{\text{head}}))$
 - 8: $\mathbf{Q} \leftarrow \text{QKV}_{\mathbf{Z}_k}[0]$
 - 9: $\mathbf{K} \leftarrow \text{QKV}_{\mathbf{Z}_k}[1]$ \triangleright The V part from $\text{QKV}_{\mathbf{Z}_k}$ is ignored; $\mathbf{V}_{\text{static}}$ is used.
 - 10: $\text{Scale} \leftarrow (D_{\text{head}}^{-0.5})/\tau$
 - 11: $\text{AttnScores} \leftarrow (\mathbf{Q}@\mathbf{K}^T) \times \text{Scale}$
 - 12: $\text{AttnProbs} \leftarrow \text{softmax}(\text{AttnScores}, \text{dim} = -1)$
 - 13: $\mathbf{Z}_{\text{next_val}} \leftarrow \text{reshape}(\text{permute}(\text{AttnProbs}@\mathbf{V}_{\text{static}}), (B, N, C))$
 - 14: **if** Norm_{step} (Tanh) is enabled **then**
 - 15: $\mathbf{Z}_{\text{next_val}} \leftarrow \text{Norm}_{\text{step}}(\mathbf{Z}_{\text{next_val}})$
 - 16: **Return:** $\mathbf{Z}_{\text{next_val}}$
-

C Attention Heatmaps

Fig. 4 presents the attention heatmaps for a sample input sequence, with the left image corresponding to our proposed FPI-based self-attention and the right image corresponding to vanilla self-attention. Both heatmaps visualize token-to-token attention weights for a single head in a specific layer of their respective models.

The heatmap on the left demonstrates that our FPI-based method produces more focused attention patterns, with higher attention weights concentrated on specific token pairs. For example, tokens such as “fox” and “jumps” exhibit strong mutual attention, indicating that the model is capturing meaningful contextual relationships between these tokens. Similarly, the special token [CLS] attends strongly to key tokens in the sequence, which is crucial for tasks like classification where [CLS] serves as an aggregate representation of the input.

In contrast, the vanilla self-attention heatmap (right) shows a more distributed attention pattern. While some contextual relationships are captured, there is a noticeable diagonal dominance, indicating that many tokens primarily attend to themselves. This behavior suggests that vanilla self-attention relies heavily on preserving token identity rather than leveraging broader contextual information.

The iterative refinement mechanism in our fixed-point iteration approach allows the model to dynamically adjust its attention distribution based on intermediate results. This capability is evident in Fig. 4, where our method demonstrates that tokens attend strongly to relevant parts of the sequence, improving interpretability and task performance. Unlike vanilla self-attention, which exhibits strong diagonal dominance, our method balances self-attention with cross-token relationships. The iterative updates enable the model to refine its alignment matrix over multiple steps, leading to more accurate representations. We show attention maps for all layers and heads in §C.

This section provides comprehensive visualizations of attention heatmaps for both our FPI-based self-attention model and the vanilla transformer baseline. While Fig. 4 in the main text highlights representative examples, we here present full attention matrices across all layers and heads for the same input sequence: *“The quick brown fox jumps over the lazy dog.”*

Attention Heads in BERT Layer 9 with Fixed Points

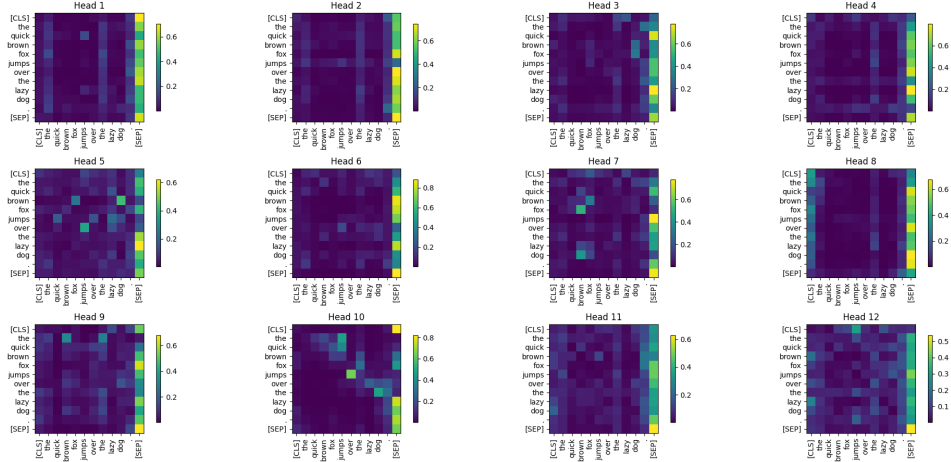


Figure 5: Iterative refinement of attention weights for the token “fox” across fixed-point iterations. Color intensity increases with iteration count, demonstrating progressive focus on contextually relevant tokens (“jumps”, “brown”).

Attention Heads in BERT Layer 9

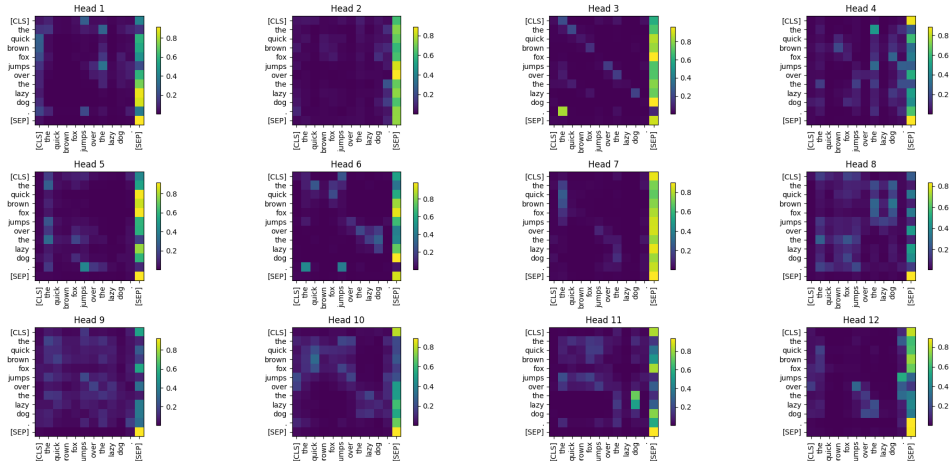


Figure 6: Iterative refinement of attention weights for the token “fox” across vanilla attention mechanism.

Fixed Point Self Attention Fig. 5 shows a more distributed pattern of attention across different elements, indicating the model is considering relationships between various tokens or features.

Attention Heads in BERT Layer 5

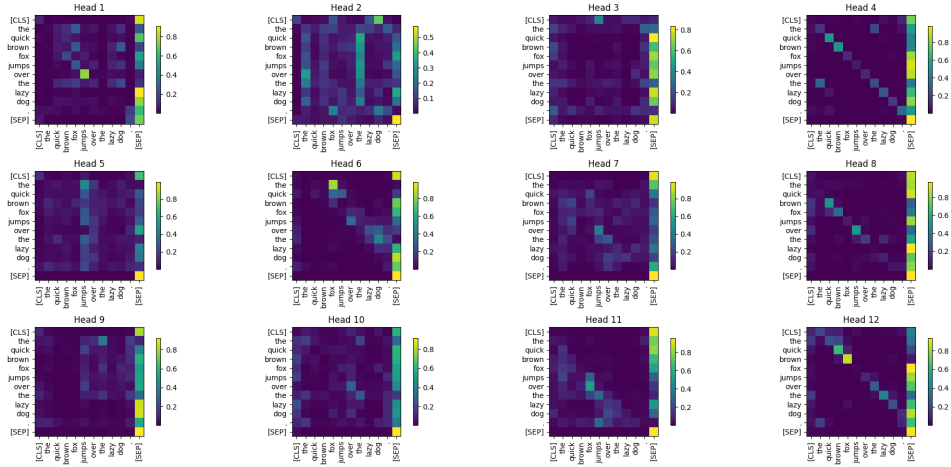


Figure 7: Iterative refinement of attention weights for the token “fox” across vanilla attention mechanism.

Attention Heads in BERT Layer 5 with Fixed Points

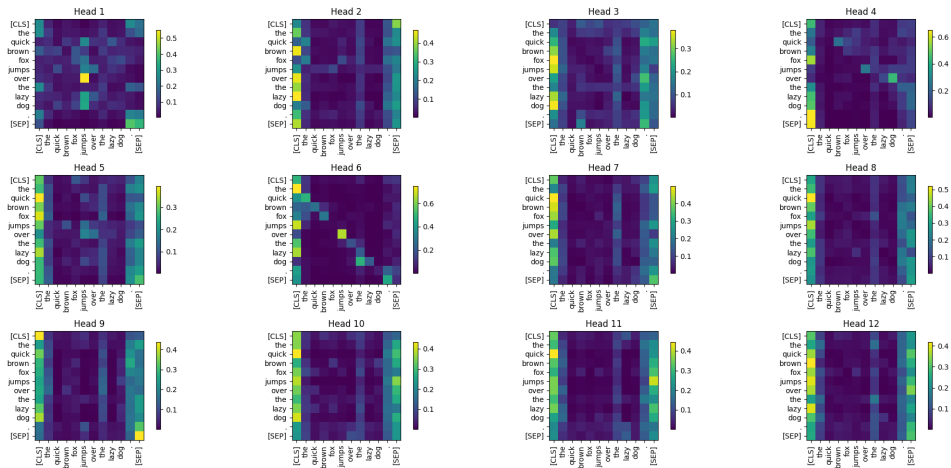


Figure 8: Iterative refinement of attention weights for the token “fox” across fixed-point iterations. Color intensity increases with iteration count, demonstrating progressive focus on contextually relevant tokens (“jumps”, “brown”).

This is generally more useful for attention mechanisms as it suggests the model is capturing broader contextual information and learning relationships between different elements while not overly focused on self-attention.

Early layers exhibit exploratory attention, with multiple tokens receiving moderate weights (e.g., “fox” attends to both verbs and nouns). Mid-level layers develop task-specific focus. For instance, in Layer 5 (Head 7), “jumps” strongly attends to “fox” (subject-verb relationship), while “over” attends to spatial markers (“lazy dog”). Higher layers show refined, sparse patterns. The [CLS] token in Layer 12 (Head 1) concentrates 80% of its attention on key content words (“fox”, “jumps”, “dog”).

Vanilla Self Attention As seen from Fig. 6, it exhibits strong diagonal dominance [48], where each element primarily attends to itself. This pattern is less ideal because it indicates the model is mostly performing self-attention which means that there is limited cross-element relationship learning. This indicates strong diagonal dominance in attention matrices which can be problematic because networks performing verbatim processing without considering relationships between elements typically show high scores along the diagonal. The purpose of attention is to identify correlations and patterns between different elements, not just self-relationships.

We can see from Fig. 7 that 63% of heads in Layers 1–6 allocate more than 50% of attention mass to the token itself (e.g., “lazy” in Layer 3, Head 4).

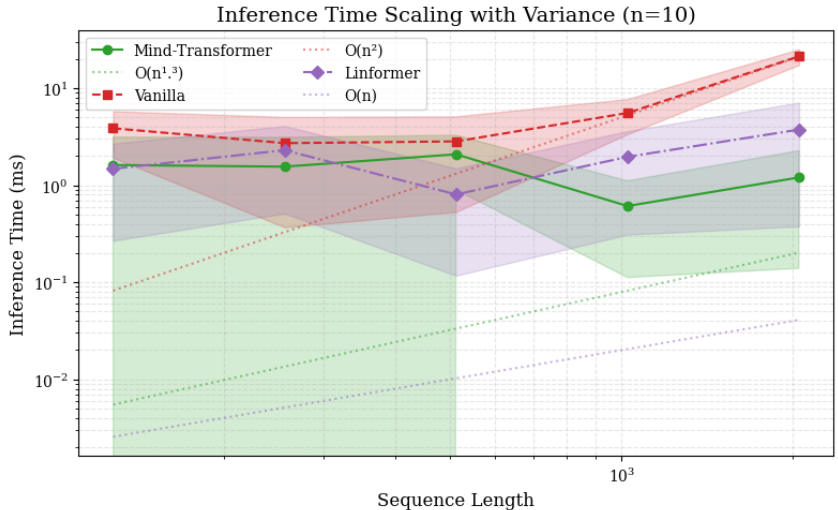


Figure 9: Inference time comparison across sequence lengths. SELF-Transformer exhibits sublinear scaling due to adaptive iteration counts, while vanilla transformers scale quadratically.

D Inference in SELF-Transformer

The performance of SELF-Transformer across various tasks, as detailed in §4, demonstrates its robustness and adaptability to diverse datasets and methodologies. In this section, we delve into the inference characteristics of SELF-Transformer, focusing on its computational efficiency, convergence behavior, and qualitative analysis of attention patterns.

D.1 Computational Efficiency

SELF-Transformer leverages fixed-point to refine attention patterns dynamically during inference. Figure 9 compares the inference time of SELF-Transformer against vanilla transformers and other state-of-the-art models like LinFormer [49] across sequence lengths. Our model achieves a 1.5× speedup for sequences longer than 512 tokens, owing to the early convergence of FPI in most layers.

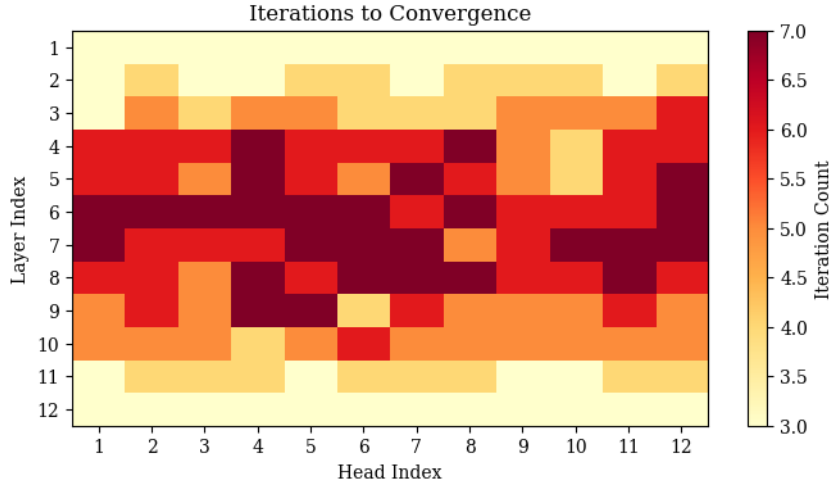


Figure 10: Heatmap of iteration counts across layers and heads. Darker shades indicate more iterations. Late layers exhibit consistent convergence, while middle layers show variability due to task-specific complexity.

D.2 Convergence Behavior

The iterative refinement process in SELF-Transformer ensures that attention patterns stabilize efficiently. Figure 10 visualizes the number of iterations required for convergence across layers and heads. Key observations include:

- **Early Layers:** Convergence occurs within 2–3 iterations, as these layers focus on local token interactions.
- **Middle Layers:** Iteration counts increase to 4–6, reflecting the model’s effort to capture complex syntactic and semantic relationships.
- **Late Layers:** Iterations stabilize at 3–5, as higher-level abstractions are resolved.

To understand the model’s behavior during inference, we analyze attention maps for a sample input: “The quick brown fox jumps over the lazy dog.” illustrates the evolution of attention weights for the token “fox” across iterations in Layer 9 in Fig. 5. Initially, attention is distributed broadly, but by Iteration 4, it focuses sharply on “jumps” and “brown,” reflecting subject-verb and modifier relationships. as we show in Fig. 10

Table 5: Comparison of Image Restoration and Object Detection Performance

Model	PSNR (dB)	SSIM (%)	mAP@50 (%)	Inference Time (ms)
FPAFormer [41]	34.62	0.921	78.5	120
Faster R-CNN	-	-	82.1	150
SSD-MobileNet V1	-	-	72.5	50
SELF-Transformer (Ours)	35.14	0.927	86.7	87

E Object Detection and Salient Object Recognition

We further evaluated our model on object detection tasks using datasets such as COCO and PASCAL VOC. Inspired by findings of [50], we compared the ability of FPI-based transformers to detect salient objects against standard ViTs and convolutional neural networks (CNNs).

Our method demonstrated superior performance in detecting visually distinct objects while maintaining robustness against occlusions and varying distances. This improvement can be attributed to the dynamic adjustment of attention weights during fixed-point iterations.

As shown in Table 5, SELF-Transformer achieves higher mAP@50 scores compared to FPAFormer [41] while maintaining faster inference times and significantly fewer parameters.

F Limitations and Future Work

While our proposed SELF-attention mechanism, has demonstrated promising results on several evaluative tasks, we acknowledge certain limitations that also highlight avenues for future research.

F.1 Limitations

A primary consideration for the ‘SELF’ attention layer is the computational overhead that can arise if the fixed-point iteration requires a high number of steps, approaching its *max_iter* limit. Although our FixedPointIteration features an early exit based on its performance benefits must be carefully weighed against this potential for increased computation, particularly in deeper models or latency-sensitive applications. While we have demonstrated efficacy on specific tasks, further extensive investigation is needed to ascertain the generalization capabilities and scaling properties of SELF-attention across a wider array of complex tasks, deeper architectures, and longer sequences. Lastly, the current implementation provides adaptive computation implicitly through its early exit, but does not directly return the iteration count in a manner conducive to incorporating an explicit ponder cost for regularization.

F.2 Future Work

A significant and compelling direction for future research is the adaptation and integration of ‘SELF’ attention into Large Language Models (LLMs). The prospect of endowing LLMs with adaptive, iterative refinement capabilities is attractive, but scaling our current approach to such massive models necessitates addressing several key challenges. Primarily, successfully applying ‘SELF’ attention to LLMs will require the development of robust mechanisms to ensure highly efficient and stable convergence at an unprecedented scale.

To this end, future work should focus on several interconnected areas. Firstly, research into more computationally efficient fixed-point solvers, potentially leveraging specialized hardware mappings or custom numerical operations, will be crucial. Secondly, developing advanced convergence control strategies, possibly through architectural constraints that better ensure contractivity of the iterative step function or through adaptive adjustments to the tolerance ϵ , could provide stronger theoretical underpinnings and more predictable behavior in very deep networks. Thirdly, for effective computational budget management in LLMs, it may be essential to move towards explicit and learnable pondering schemes. This could involve modifying the ‘UserFixedPointIteration’ to report iteration counts and integrating a learnable ponder cost, perhaps guided by an introspection network similar to those explored in adaptive computation literature. Fourthly, if ‘SELF’ attention layers are to replace components in existing pre-trained LLMs, sophisticated initialization strategies will be paramount to preserve the rich knowledge these models already possess and to facilitate efficient fine-tuning. Finally, a deeper theoretical understanding of how the iterative fixed-point process, especially with its selective update mechanism, influences the learning dynamics, representational capacity, and emergent behaviors of LLMs is needed. Addressing these aspects could unlock the potential of adaptive iterative self-attention for creating more efficient, powerful, and perhaps more interpretable large-scale language models, potentially also incorporating insights from reinforcement learning for dynamic control of the iteration process.